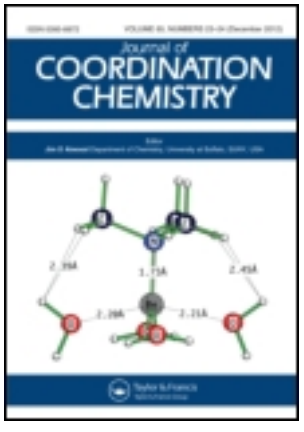

Journal of Coordination Chemistry
Publication details, including instructions for authors and subscription information:
http://www.tandfonline.com/loi/gcoo20

Synthesis, crystal structures, and selected properties of Cu(II) and Zn(II) complexes with in situ formed 2-hydroxy-N′-(propan-2-ylidene)benzohydrazide

Shunsheng Zhao [a], Sijiao Wang [a], Xiangrong Liu [a], Bei Liang [a], Lanlan Li [a], Huiwu Cai [a] & Kanshe Li [a]

[a] College of Chemistry and Chemical Engineering, Xi'an University of Science and Technology, 710054, Xi'an, P.R. China

Accepted author version posted online: 11 Oct 2012.Published online: 30 Oct 2012.

To cite this article: Shunsheng Zhao, Sijiao Wang, Xiangrong Liu, Bei Liang, Lanlan Li, Huiwu Cai & Kanshe Li (2012) Synthesis, crystal structures, and selected properties of Cu(II) and Zn(II) complexes with in situ formed 2-hydroxy-N′-(propan-2-ylidene)benzohydrazide, Journal of Coordination Chemistry, 65:24, 4277-4287, DOI: 10.1080/00958972.2012.738813

To link to this article: http://dx.doi.org/10.1080/00958972.2012.738813

Journal of Coordination Chemistry
Vol. 65, No. 24, 20 December 2012, 4277–4287

Synthesis, crystal structures, and selected properties of Cu(II) and Zn(II) complexes with *in situ* formed 2-hydroxy-N′-(propan-2-ylidene)benzohydrazide

SHUNSHENG ZHAO, SIJIAO WANG, XIANGRONG LIU*, BEI LIANG, LANLAN LI, HUIWU CAI and KANSHE LI

College of Chemistry and Chemical Engineering, Xi'an University of Science and Technology, 710054 Xi'an, P.R. China

(*Received 12 April 2012; in final form 7 September 2012*)

$Cu(C_{10}H_{11}O_2N_2)_2$ (**1**) and $[Zn(C_{10}H_{12}O_2N_2)_2(H_2O)_2](NO_3)_2$ (**2**) were synthesized and characterized by elemental analysis, FT-IR spectra, UV-Vis absorption spectroscopy, and X-ray single-crystal diffraction. Both complexes show distorted octahedral geometry. In **1**, Cu(II) is coordinated by four oxygen atoms from four ligands and two nitrogen atoms from two ligands. In **2**, Zn(II) is coordinated by two oxygen atoms and two nitrogen atoms from two ligands, and two water molecules. The crystal structures suggest that original ligand o-carboxybenzaldehyde salicyloylhydrazone ($C_{15}H_{12}O_4N_2$) changed into acetone salicyloylhydrazone ($C_{10}H_{12}O_2N_2$). The TG-DTG curves of these complexes indicate two different decomposition processes. **1** and **2** display catalytic activities to decomposition of hydrogen peroxide. Interaction between the complexes and DNA studied by UV-Vis titration shows the insert interaction.

Keywords: Synthesis; Crystal structure; Complex; Thermal behavior; DNA Binding ability

1. Introduction

Biological applications of inorganic pharmaceuticals play a key role in clinical therapy. Examples include cis-platin and corresponding second generation alternatives such as oxaliplatin and carboplatin serving as chemotherapeutic agents for tumors and as diagnostic contrast agents such as MRI [1–3]. Transition metals are particularly suitable for this purpose in that they can adopt a wide variety of coordination numbers, geometries, and oxidation states in comparison with carbon and other main group elements [4].

Our interest was attracted to transition metal complexes of acyl hydrazones because acyl hydrazones have been reported to function as antibacterial, antiviral, antifungal, and antitumor agents, and for DNA interactions and cleavage [5–8]. Coordination of bioactive ligands to metal may increase their activity and some bioinactive ligands acquire activity through coordination. Many complexes derived from hydrazones have biological activities and are pharmacologically important.

*Corresponding author. Email: xkchemistry@yahoo.com.cn

ISSN 0095-8972 print/ISSN 1029-0389 online
http://dx.doi.org/10.1080/00958972.2012.738813

Interactions of DNA with small molecules can serve as a foundation for design of new types of pharmaceutical molecules. Interaction models of transition metal complexes with DNA and their subsequent applications in molecular biology attract attention. In particular, interest has been generated in DNA binding and DNA cleavage by redox and photoactive metal complexes in order to explore sequence specificities of DNA binding using intercalating ligands [9–11].

There is no literature available on the synthesis, structural characterization, and interaction studies of Cu(II) and Zn(II) complexes containing 2-hydroxy-N′-(propan-2-ylidene)benzohydrazide, stimulating our interest in synthesis, structure, DNA binding, cleavage, protein binding, and antioxidant properties of Cu and Zn complexes containing the above hydrazone. Structures of the new complexes were established by single-crystal X-ray diffraction and spectroscopic data. In addition, investigations on thermal decomposition of the complexes and their catalytic activity in the decomposition of hydrogen peroxide were also undertaken.

2. Experimental

2.1. *Measurements*

Elemental analyses were carried out on a P.E.2400-II instrument. IR spectra were recorded on a P.E.983 FT-IR spectrophotometer with KBr pellets. UV-Vis spectra were obtained on a TU-1900 spectrophotometer using DMF as solvent at $10^{-5}\,\mathrm{mol\,L^{-1}}$. Crystal structures were determined using a Bruker SMART APEX CCD diffractometer equipped with graphite monochromated Mo-Kα radiation ($\lambda = 0.\ 71\,073$ Å). Thermal data were collected on a Q1000DSC + LNCS + FACS Q600SDT instrument in nitrogen at heating rates of 5°C, 10°C, and 15°C min^{-1} from 30°C to 800°C.

2.2. *Materials and synthesis*

All chemicals are reagent grade and used as purchased without purification. The CT-DNA was purchased from Sigma Company. CT-DNA was dissolved in Tris-HCl buffer ($0.1\,\mathrm{mol\,L^{-1}}$, pH = 7.25). 2-((Salicyloylhydrazono)methyl)benzoic acid was prepared according to a previously reported method [12].

2.2.1. Synthesis of bis[2-hydroxy-N′-(propan-2-ylidene)benzohydrazonato]copper(II) (1). To a solution of $Cu(NO_3)_2 \cdot 3H_2O$ (0.11 g, 0.4 mmol) in DMF (10 mL), a solution of the 2-((salicyloylhydrazono)methyl)benzoic acid (0.23 g, 0.8 mmol) in DMF (10 mL) was added. The color of the reaction mixture changed from blue to green. The mixture was stirred at 50°C in a water bath for 1 h. An aliquot of the resulting solution was analyzed to determine the complex formed. The remaining solution was kept in a sealed bottle containing acetone, allowing acetone to slowly evaporate at room temperature. Dark green crystals of $Cu(C_{10}H_{11}O_2N_2)_2$ were obtained 2 weeks later. The crystals were collected by filtration, washed with methanol, and finally dried. Anal. Calcd for $Cu(C_{10}H_{11}O_2N_2)_2$ (%): C, 53.86; H, 4.97; N, 12.56; O, 14.35. Found (%): C, 53.81; H, 4.85; N, 12.55; O, 15.58.

Table 1. Crystallographic data for **1** and **2**.

	1	**2**
Empirical formula	$C_{20}H_{22}N_4O_4Cu$	$C_{20}H_{28}N_6O_{12}Zn$
Formula weight	445.96	609.85
Crystal color	Dark green	Yellow
Crystal system	Monoclinic	Monoclinic
Space group	$P2(1)/n$	$P2(1)/n$
Unit cell dimensions (Å, °)		
a	6.2989(10)	7.456(4)
b	16.085(3)	9.943(5)
c	9.7177(15)	17.198(8)
β	97.241(2)	98.098(8)
Volume (Å^3), Z	976.7(3), 2	1262.2(10), 2
Calculated density (Mg m^{-3})	1.516	1.605
Absorption coefficient (mm^{-1})	1.153	1.048
$F(000)$	462	632
Crystal size (mm^3)	$0.31 \times 0.27 \times 0.15$	$0.33 \times 0.27 \times 0.14$
θ range for data collection (°)	2.46–25.10	2.37–25.09
Limiting indices	$-7 \le h \le 6$; $-19 \le k \le 15$; $-9 \le l \le 11$	$-8 \le h \le 8$; $-11 \le k \le 11$; $-20 \le l \le 14$
Reflections collected/unique	4819/1737	5908/2229
Independent reflection	[R(int) = 0.0199]	[R(int) = 0.0629]
Goodness-of-fit on F^2	1.098	0.999
R indices [$I > 2\sigma(I)$] R_1, wR_2	0.0273, 0.0776	0.0676, 0.1711
R indices (all data) R_1, wR_2	0.0340, 0.0814	0.0831, 0.1786

2.2.2. Synthesis of {bis[2-hydroxy-N′-(propan-2-ylidene)benzohydrazide]}(dihydrato) zinc(II) nitrate (2). This complex was prepared by reacting a CH_2Cl_2 (7 mL) solution of $Zn(NO_3)_2 \cdot 6H_2O$ (0.15 g, 0.4 mmol) with a DMF (7 mL) solution of 2-((salicyloylhydrazono)methyl)benzoic acid (0.23 g, 0.8 mmol) at 50°C in a water bath for 1 h. An aliquot of the resulting solution was analyzed to determine the complex formed. The remaining solution was kept in a sealed bottle containing acetone and the acetone slowly evaporated at room temperature. After 2 weeks, yellow crystals appeared. The crystals were collected by filtration, washed with methanol and finally dried. Anal. Calcd for $[Zn(C_{10}H_{12}O_2N_2)_2(H_2O)_2](NO_3)_2$ (%): C, 39.39; H, 4.63; N, 13.78; O, 31.48. Found (%): C, 39.35; H, 4.62; N, 13.56; O, 31.37.

2.2.3. Crystallographic studies. Crystallographic information for **1** and **2** is listed in table 1. Determination of unit cell parameters and data collections were performed with Mo-Kα radiation ($\lambda = 0.71073$ Å). The structures were solved by direct methods and semi-empirical absorption correction using SHELXTL-97. Non-hydrogen atoms were located with difference Fourier synthesis and hydrogen atoms were generated geometrically. The CCDC reference numbers for **1** and **2** are 721329 and 733609, respectively.

2.2.4. Decomposition of hydrogen peroxide. A mixture of **1** (1 mL, 1 mol L^{-1}) and hydrogen peroxide (20 mL, 15%) was put aside for 1 d (20°C), then the hydrogen peroxide left was titrated with potassium permanganate standard solution and the percentage of the hydrogen peroxide decomposition was calculated according to the titration result. Method used for **2**, ligand, copper nitrate, or zinc nitrate was same as that for **1**.

2.2.5. Interaction of CT-DNA. Mixed solutions of **1** (1.0×10^{-4} mol L^{-1}) and DNA (various concentrations) in buffer solution (pH = 7.3) were put aside for 30 min and then UV-Vis absorption spectra were measured at room temperature. The method used for **2** was the same as that for **1**.

3. Results and discussion

3.1. *Structure description*

3.1.1. *In situ* characterization of bis(N′-2-carboxybenzylidene-2-hydroxybenzohydrazonato)copper(II), intermediate a. For the preparation of **1**, a green reaction solution is obtained when mixing DMF solution of ligand (colorless) and copper nitrate (blue). Molar conductivity measurement (11.3 S m^2 mol^{-1}) of the resulting reaction solution indicates that intermediate **a** exists as a non-electrolyte [13]. Existence of phenolic ($\delta = 11.79$ ppm) and carboxylic group ($\delta = 13.87$ ppm) protons in ^{1}H-NMR spectrum of the complex solution demonstrates the proposed structure with amide group deprotonated. Comparing to the ligand, the band of the azomethine $n \rightarrow \pi^*$ transition in UV-Vis absorption spectra of the reaction solution shifts to lower frequencies, also indicating that the imine nitrogen is involved in coordination. When acetone is allowed to penetrate slowly into the solution, the o-carboxybenzaldehyde in intermediate **a** is replaced by acetone with coordination bonds unbroken. Similar ligand reactions with coordination bond unbroken could be found in the previous report [14].

3.1.2. *In situ* characterization of [bis(N′-2-carboxybenzylidene-2-hydroxybenzohydrazide)(dihydrato)]zinc(II), intermediate b. In contrast with **1**, for **2**, the solution remains colorless when mixing DMF solution of ligand (colorless) and zinc nitrate (colorless). Molar conductivity measurement (219.1 S m^2 mol^{-1}) of the reaction solution indicates that intermediate **b** exists as a bivalent electrolyte, which suggests the complex cation with neutral ligands and two accompanying NO_3^-. ^{1}H-NMR spectrum of the complex solution shows existence of phenolic ($\delta = 11.73$ ppm), carboxylic ($\delta = 13.09$ ppm), and amide ($\delta = 2.15$ ppm) protons, consistent with the proposed structure of intermediate **b**. When acetone is allowed to penetrate slowly into the solution, the o-carboxybenzaldehyde in intermediate **b** is replaced by acetone with coordination bonds unbroken, consistent with the reaction in formation of **1**.

3.1.3. Structure description of 1. The crystal structure and packing diagram of **1** are shown in figures 1 and 2, respectively. Selected bond lengths and angles are listed in table 2. Hydrogen bonding geometry is given in table 3.

As figure 2 and table 2 show, each Cu(II) adopts a distorted octahedral geometry in which the basal plane is formed by coordination of two imino nitrogen atoms and two carbonyl oxygen atoms from two ligands; the axial sites are occupied by two phenolic hydroxyl oxygen atoms from two other ligands with a relatively weak interaction.

The bond lengths of Cu–O and Cu–N are in agreement with previously reported data of complexes with similar structures [15–17]. Cu–O bond length (1.903 Å) is a little shorter than that of Cu–N, which means oxygen has better coordination ability with

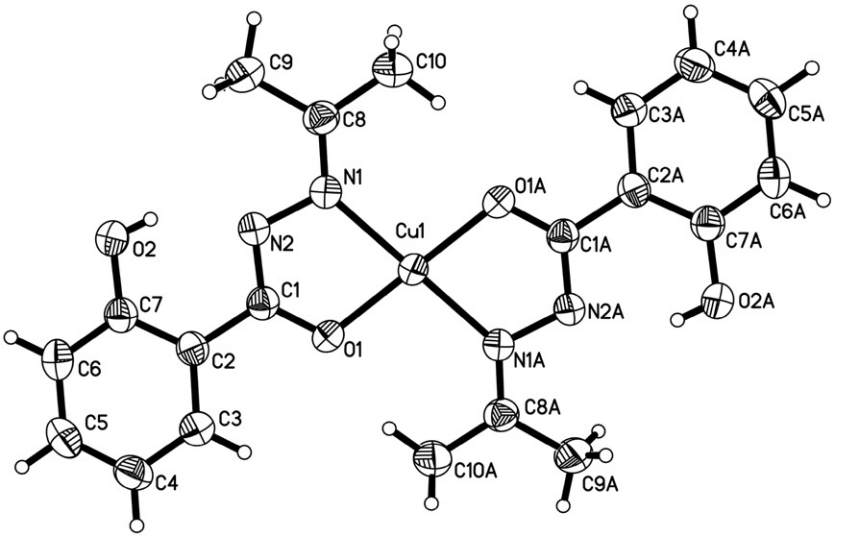

Figure 1. Crystal structure of **1** (symmetry transformations used to generate equivalent atoms: A $-x-2$, $-y+1$, $-z$).

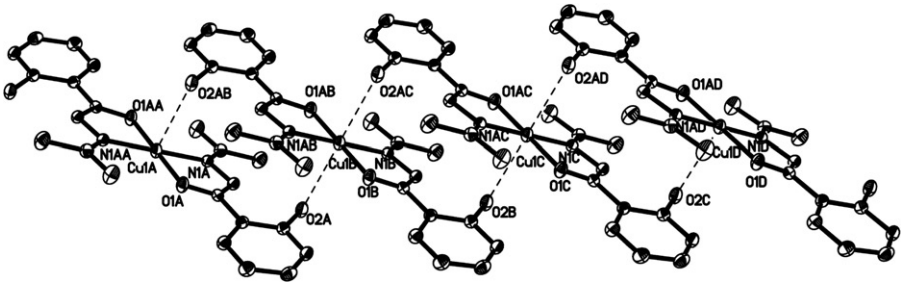

Figure 2. Layer structure of **1** (symmetry transformations used to generate equivalent molecules: A x, y, z; B $x+1, y, z$; C $x+2, y, z$; D $x+3, y, z$; AA $-x-2, -y+1, -z$; AB $-x-1, -y+1, -z$; AC $-x, -y+1, -z$; AD $-x+1, -y+1, -z$).

Cu(II) than does nitrogen [18]. The two five-membered chelate rings are essentially planar (Cu1–N1–N2–C1–O1 and Cu1–N1A–N1A–C1A–O1A). The C1–N2 bond length is 1.319(3) Å, shorter than that of C–N single bond (1.47 Å) but longer than that of C=N double bond (1.273 Å), due to conjugation between C=O and C=N. The O1–C1 bond length is 1.285(2) Å, between C=O double bond (1.233 Å) and C–O single bond (1.336 Å). Inter-unit coordination of metals and ligands from different unsymmetrical units makes **1** a coordination polymer and stacking interaction induces the *z*-type 3-D structure, as shown in figure 2.

3.1.4. Structure description of 2. In **2**, the Zn(II) is six coordinate with a distorted octahedral geometry. The crystal structure and layer structure are shown in figures 3 and 4. The six-coordinate groups are two imino nitrogen atoms and two

Table 2. Selected bond lengths (Å) and angles (°) for **1** and **2**.

1		**2**	
Cu(1)–O(1)#1	1.9029(14)	Zn(1)–O(1)	2.050(3)
Cu(1)–O(1)	1.9029(14)	Zn(1)–O(1)#2	2.050(3)
Cu(1)–N(1)#1	2.0547(18)	Zn(1)–N(1)	2.193(3)
Cu(1)–N(1)	2.0547(18)	Zn(1)–N(1)#2	2.193(3)
Cu(1)–O(2)#3	2.7561(17)	Zn(1)–O(2)	2.102(3)
Cu(1)–O(2)#4	2.7561(17)	Zn(1)–O(2)#2	2.102(3)
N(1)–C(8)	1.288(3)	N(1)–C(2)	1.276(5)
N(1)–N(2)	1.402(2)	N(1)–N(2)	1.385(5)
N(2)–C(1)	1.319(3)	N(2)–C(4)	1.335(5)
O(1)–C(1)	1.285(2)	N(3)–O(6)	1.205(5)
O(2)–C(7)	1.363(3)	N(3)–O(4)	1.221(5)
O(1)#1–Cu(1)–O(1)	180.0	O(1)#2–Zn(1)–O(1)	180.0
O(1)#1–Cu(1)–N(1)#1	80.83(6)	O(1)#2–Zn(1)–N(1)#2	76.54(12)
O(1)–Cu(1)–N(1)#1	99.17(6)	O(1)–Zn(1)–N(1)#2	103.46(13)
O(1)#1–Cu(1)–N(1)	99.17(6)	O(1)#2–Zn(1)–N(1)	103.46(13)
O(1)–Cu(1)–N(1)	80.83(6)	O(1)–Zn(1)–N(1)	76.54(12)
N(1)#1–Cu(1)–N(1)	180.00(8)	N(1)#1–Zn(1)–N(1)	180.000(1)
O(2)#3–Zn(1)–O(2)#4	180.00(5)	O(2)–Zn(1)–O(2)#2	180.0(2)
O(2)#3–Cu(1)–N(1)	88.298(55)	O(2)–Zn(1)–N(1)	88.19(15)
O(2)#3–Cu(1)–O(1)	91.785(58)	O(2)–Zn(1)–O(1)	88.91(15)

Symmetry transformations used to generate equivalent atoms: #1 $-x-2, -y+1, -z$; #2 $-x, -y, -z+1$; #3 $x-1, y, z$; #4 $-x-1, -y+1, -z$.

Table 3. Hydrogen bonding geometry (Å, °).

	D–H···A	d (D–H)	d (H···A)	d (D···A)	∠(DHA)
1	O(2)–H(2A)···N(2)	0.77(2)	1.90(2)	2.579(2)	148(2)
2	N(2)–H(2)···O(3)	0.86	1.90	2.576	134.3
	O(3)–H(3)···O(5)#5	0.82	1.86	2.665	169.2
	O(2)–H(2A)···O(4)	0.87	1.92	2.770	163.7
	O(2)–H(2B)···O(5)#6	0.85	1.87	2.720(5)	174.9

Symmetry transformations used to generate equivalent atoms: #5 $-x+1, -y+1, -z+1$; #6 $-x+1, -y, -z+1$.

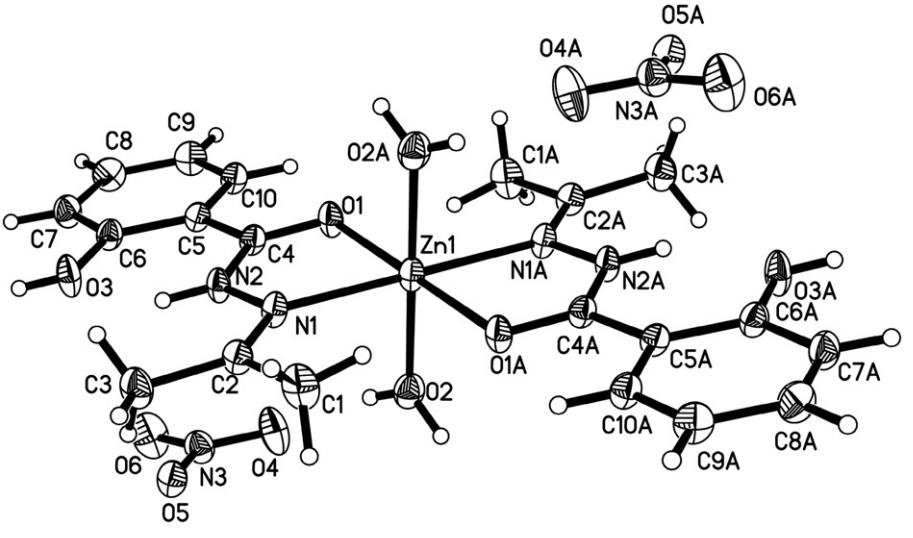

Figure 3. Crystal structure of **2** (symmetry transformations used to generate equivalent atoms: A $-x, -y, -z+1$).

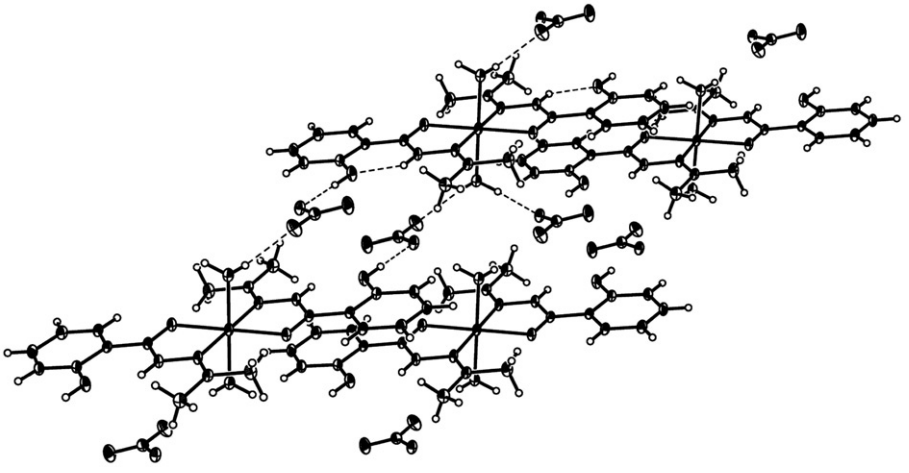

Figure 4. Layer structure of **2**.

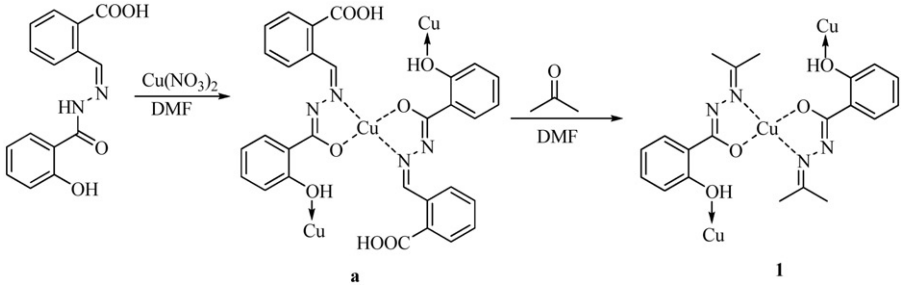

Scheme 1. Formation of **1**.

carbonyl oxygen atoms from two ligands. There are also two water molecules occupying the axial sites.

The average Zn–O and Zn–N bond lengths are 2.076 Å and 2.193(3) Å, respectively, similar with previous reports [19–21]. The five-membered chelate rings (Zn1–N1–N2–C4–O1 and Zn1–N1A–N2A–C4A–O1A) are in one plane. The N1–C2 bond length is 1.275(5) Å, similar with a C=N (1.273 Å). The O1–C4 bond length is 1.246(5) Å, close to C=O double bond length (1.233 Å). The intramolecular hydrogen bond N2–H2···O3 (2.576 Å, 134.3°) stabilizes the planarity of the ligand in the complex. Intermolecular hydrogen bonds (O3–H3···O5 and O2–H2···O5) link the complex cations and nitrate anions to form layers. These flat layers are interconnected by hydrogen bonds between water and NO_3^- to form a network.

3.2. *The formation mechanisms of 1 and 2*

The formation mechanisms of the complexes are proposed through intermediates **a** and **b**, respectively. Substitution occurs when acetone is allowed to penetrate slowly into the solution to give **1** and **2**, as shown in schemes 1 and 2.

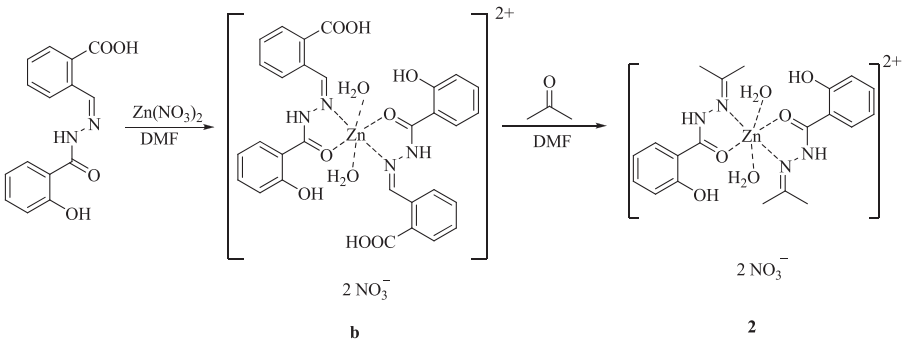

b 2

Scheme 2. Formation of **2**.

3.3. *IR spectra*

The IR spectrum of ligand shows bands at 1606 and 1662 cm^{-1} assigned to υ(C=N) and υ(C=O), respectively. Moreover, in the IR spectrum of **1** ("Supplementary material"), υ(C=N) and υ(C=O) shift to 1555 υ(C=N) and 1605 cm^{-1} υ(C=O), and υ(OH/NH, enol/keto) disappears due to coordination [22, 23]. In the IR spectrum of **2**, υ(C=N) and υ(C=O) shift to 1567 υ(C=N) and 1622 cm^{-1} υ(C=O) and an OH vibration could be assigned to coordinated water. A strong band at 1380 cm^{-1} in **2** indicates the existence of non-coordinated nitrate, also evidenced by single-crystal X-ray diffraction.

3.4. *UV-Vis absorption spectra*

The ligand and complexes in DMF (10^{-5} mol L^{-1}) show absorptions between 200 and 500 nm. The free ligand exhibits a strong absorption at 322 nm, due to intraligand π–π^* transition. In **1** and **2**, spectra show intense bands at 311 and 313 nm, respectively, which can be assigned to π–π^* transitions. The azomethine $n \rightarrow \pi^*$ band is shifted to lower frequencies, indicating that the imine nitrogen is coordinated to metal [24].

3.5. *Thermal analysis*

TG-DTG curves of **1** and **2** at 10°C min^{-1} are shown in "Supplementary material." TG–DTG curves at 5°C min^{-1} and 15°C min^{-1} are similar with that of 10°C min^{-1}. Weight losses and corresponding temperature ranges of the complexes during decomposition are obtained from these figures.

From figure S2 for **1**, there are two distinct stages in decomposition. The first from 100°C to 280°C with a mass loss of 60.0% (Calcd 60.35%) is connected with loss of the phenol and two methyls. The second decomposition stage occurs from 280°C to 600°C with a mass loss of 22.24% (Calcd 21.99%), assigned to loss of two five-membered chelate rings. The remainder, probably CuO, has mass of 16.73% as against the calculated value of 17.76%.

For **2**, there are three stages in the decomposition ("Supplementary material"). The first stage from 35°C to 170°C with a mass loss of 12.88% (Calcd 13.19%) is connected with the loss of coordinated water. The second stage occurs from 170°C to 340°C, assigned to loss of nitrate and two methyls with a mass loss of 25.00% (Calcd 26.70%).

Table 4. The catalytic properties of compound for decomposition of hydrogen peroxide.

Compound	Decomposition percent of H_2O_2 (%)
$Cu(NO_3)_2 \cdot 3H_2O$	90.5
$Zn(NO_3)_2 \cdot 6H_2O$	80.2
Ligand	85
Complex **1**	99.8
Complex **2**	96.7

The third stage, from 340°C to 800°C, with a mass loss of 32.82% (Calcd 34.08%), is assigned to loss of phenol. When the temperature is 800°C, the remaining mass of 29.1% could be assigned to Zn and coordinated atoms (Calcd 29.5%). This indicates that **2** decomposes incompletely at 800°C.

3.6. *The catalytic activity of 1 and 2*

The test of catalytic decomposition activity to hydrogen peroxide shows that **1** and **2** have good catalytic activity (table 4). In the same concentration of the catalyst, the metal salts and their complexes have catalytic decomposition activity. The ligand also has some catalytic activity. The complexes perform much better catalytic ability than corresponding salts and ligand.

3.7. *DNA binding study*

UV-Vis spectroscopy is an effective method for examining the binding of DNA with metal complexes [26]. The potential binding abilities of ligand, **1** and **2** to CT-DNA were studied by UV-Vis absorption spectroscopy. Figure 5 and figures S4 and S5 (“Supplementary material”) show the intensity variation of intraligand π–π^* transition of the ligand, **1** and **2** upon addition of CT-DNA with an increasing concentration. Hypochromism of 11% for ligand, 3% for **1** and 1% for **2** was observed (table 5). Although this is not definitive, hypochromism observed for other complexes in the presence of CT-DNA is taken as a sign of an intercalative binding mode, where stacking interactions between the aromatic chromophore of the complex and the base pairs of DNA modulate the absorption characteristics of the metal complexes [27]. Comparing with previous reports [28], we proposed that the hypochromism observed in UV spectra is due to the partial/moderate intercalation of the ligand within the complexes. The extent of the hypochromism is commonly consistent with the strength of intercalative interaction. Our results imply that our ligand is similar to TACN [28] and bpa-R [29], which do not intercalate very strongly or deeply between the DNA base pairs.

4. Conclusion

Two complexes with same coordination geometry were synthesized and characterized. The structures of the complexes show original ligand changed into acetone

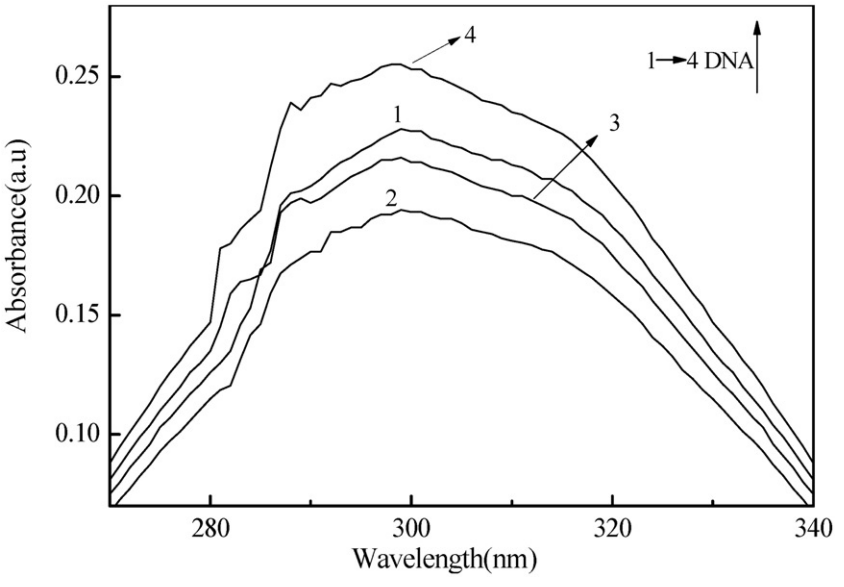

Figure 5. Changes in the absorption spectra of **1** on titration with increasing CT-DNA concentration (0–50 μmol L^{-1}).

Table 5. The changes of the UV-Vis spectrum after interaction between compounds and DNA.

	λ_{max} (nm)			
Compound	Free state	Bound state	Δλ	Absorbance changes (%)
Ligand	322	298	−24	11
Complex **1**	311	299	−12	3
Complex **2**	313	300	−13	1

salicyloylhydrazone and the nitrate in **2** is not coordinated. Thermal decomposition of **1** is divided into two stages, while **2** is divided into three stages. Catalytic activity to decomposition of hydrogen peroxide shows that **1** displays better activity than **2**. The modes of CT-DNA binding to ligand, **1** and **2** have been proposed as moderate intercalation.

Supplementary material

CCDC 721329 and 733609 contain the supplementary crystallographic data for **1** and **2**. The data can be obtained free of charge from the Cambridge Crystallographic Data Centre *via* www.ccdc.cam.ac.uk/conts/retrieving.html.

Acknowledgments

The authors are grateful to National Natural Science Foundation of China (Nos. 21073139, 21103135, and 51173145), Scientific Research Program Funded by Shaanxi Provincial Education Commission (Nos. 07JK317 and 12JK0622), Natural Science Basic Research Plan in Shaanxi Province of China (No. 2011JQ2011), the Open Foundation of the Laboratory of Space Materials Science and Technology of NWPU, and Cultivation Foundation of Xi'an University of Science and Technology (Program No. 2010QJD030) for supporting this research.

References

[1] L. Ranconi, P.J. Sadler. *Coord. Chem. Rev*., **251**, 1633 (2007).
[2] T. Storr, K.H. Thompson, C. Orvig. *Chem. Soc. Rev*., **35**, 534 (2006).
[3] Z. Guo, P.J. Sadler. *Angew. Chem. Int. Ed*., **38**, 1512 (1999).
[4] G.L. Miessler, D.A. Tarr. *Inorganic Chemistry*, 3rd Edn, p. 299, Prentice Hall, New Jersey (2003).
[5] N.A. Mangalam, M.R.P. Kurup. *Spectrochim. Acta, Sect. A*, **78**, 926 (2011).
[6] P. Krishnamoorthy, P. Sathyadevi, K. Senthilkumar, P.T. Muthiah, R. Ramesh, N. Dharmaraj, Y. Okazaki. *Inorg. Chem. Commun*., **314**, 71318 (2011).
[7] D.S. Raja, N.S.P. Bhuvanesh, K. Natarajan. *J. Biol. Inorg. Chem*., **17**, 223 (2012).
[8] S. Mukherjee, S. Chowdhur, A.P. Chattapadhyay, A. Bhattacharya. *Inorg. Chim. Acta*, **373**, 40 (2011).
[9] J.K. Barton. *Science*, **233**, 727 (1986).
[10] J.C. Francois, T. Saison-Behmoaras, M. Chassignol, N.T. Thuong, J.S. Sun, C. Helene. *Biochemistry*, **27**, 2272 (1988).
[11] Q. Guo, M. Lu, N.C. Seeman, N.R. Kallenbach. *Biochemistry*, **29**, 570 (1990).
[12] B. Liang, X.R. Liu, P.H. Zhang. *Chin. J. Org. Chem*., **30**, 1580 (2010).
[13] J. Geary. *Coord. Chem. Rev*., **7**, 81 (1971).
[14] F. Yang, J.J. Lin, Y.K. Shan. *Coordination Chemistry*, East China Normal University Press, China (2002) (in Chinese).
[15] L.M. Wu, G.F. Qiu, H.B. Teng. *Inorg Chim. Acta*, **360**, 3069 (2007).
[16] A.A. Khandar, K. Nejati. *Polyhedron*, **19**, 607 (2000).
[17] J. Jaskova, D. Miklos, M. Korabik. *Inorg. Chim. Acta*, **360**, 2771 (2007).
[18] R.B. King. *Encyclopedia of Inorganic Chemistry*, **8**, 29 (1994).
[19] M. Đaković, M. Vinković, S. Roca, Z. Popović, I. Vicković, D. Vikić-Topić, J. Lukač, N. Đaković, Z. Kusić. *J. Coord. Chem*., **65**, 1017 (2012).
[20] J.L. Huang, H. Su. *Chin. J. Inorg. Chem*., **4**, 722 (2009).
[21] X.H. Chen, Q.J. Wu. *Chin. J. Inorg. Chem*., **5**, 912 (2009).
[22] A. Ray, S. Banerjee, R.J. Butecher. *Polyhedron*, **27**, 2409 (2008).
[23] S. Gupta, S. Pal, A.K. Barik, A. Hazra. *Polyhedron*, **17**, 2519 (2008).
[24] J.H. Chang, Q.G. Dong. *Principle and Analysis of Spectral*, 2nd Edn, Science Press, China (2005) (in Chinese).
[25] R.Z. Hu, S.L. Gao, F.Q. Zhao, Q.Z. Shi, T.L. Zhang, J.J. Zhang. *Thermal Analysis Kinetics (II)*, p. 79, Science Press, Beijing (2008) (in Chinese).
[26] H.P. Yang, W.H. Zhang, Q.X. Zhao. *Chin. J. Inorg. Chem*., **22**, 488 (2006).
[27] M.S. Deshpande, A.A. Kumbhar, A.S. Kumbhar. *Inorg. Chem*., **46**, 5450 (2007).
[28] J. Qian, L.P. Wang, J.L. Tian, C.Z. Xie, S.P. Yang. *J. Coord. Chem*., **65**, 122 (2012).
[29] G.F. Qi. *Transition Met. Chem*., **32**, 233 (2007).